Characterization of human PA2.26 antigen (T1α–2, podoplanin), a small membrane mucin induced in oral squamous cell carcinomas

Ester Martín-Villar[1], Francisco G. Scholl[1, 4], Carlos Gamallo[2], Maria M. Yurrita[1], Mario Muñoz-Guerra[3], Jesús Cruces[1] and Miguel Quintanilla[1 *]

[1]Instituto de Investigaciones Biomédicas Alberto Sols, Consejo Superior de Investigaciones Científicas (CSIC)-Universidad Autónoma de Madrid (UAM), Arturo Duperier 4, 28029-Madrid, Spain.

[2]Department of Pathology, Hospital Universitario de la Princesa, Facultad de Medicina, UAM, Madrid, Spain.

[3]Department of Oral and Maxillofacial Surgery, Hospital Universitario de la Princesa, Madrid, Spain.

[4]Present address: Columbia University, Department of Physiology and Cellular Biophysics, College of Physicians and Surgeons, Center for Neurobiology and Behavior, New York 10032.

[*]To whom correspondence should be addressed

Instituto de Investigaciones Biomédicas Alberto Sols, C/Arturo Duperier nº 4, 28029 Madrid, Spain. Fax: +34-91-585-44-01. E-mail: mquintanilla@iib.uam.es

Key words: mucin; PA2.26; ezrin; E-Cadherin; microvilli; OSCC

Short title: PA2.26 antigen and oral squamous cell carcinoma

Abbreviations: SCC, squamous cell carcinoma; OSCC, oral SCC; EST, expressed sequence tag; UTR, untranslated region; ORF, open reading frame; Ab, antibody; mAb, monoclonal Ab; ERM, ezrin, radixin, moesin.

Summary

We report the full cDNA sequence encoding the human homologue of murine PA2.26 (T1α-2, podoplanin), a small mucin-type transmembrane glycoprotein originally identified as a cell-surface antigen induced in keratinocytes during mouse skin carcinogenesis. The human *PA2.26* gene is expressed as two transcripts of 0.9- and 2.7-kb in several normal tissues, such as the placenta, skeletal muscle, heart and lung. Using a specific polyclonal antibody raised against a synthetic peptide of the protein ectodomain, PA2.26 was immunohistochemically detected in about 25% (15/61) of human early oral squamous cell carcinomas. PA2.26 distribution in the tumours was heterogeneous and often restricted to the invasive front. Double immunofluorescence and confocal microscopy analysis showed that PA2.26 colocalized with the membrane cytoskeleton linker ezrin at the surface of tumour cells, and that its presence *in vivo* was associated with downregulation of membrane E-cadherin protein expression. Ectopic expression of human PA2.26 in HeLa carcinoma cells and immortalized HaCaT keratinocytes promoted a redistribution of ezrin to the cell edges, the formation of cell-surface protrusions, and reduced Ca^{2+}-dependent cell-cell adhesiveness. These results point to PA2.26 as a novel biomarker for oral squamous cell carcinomas, that might be involved in migration/invasion.

Introduction

Squamous cell carcinomas (SCCs) of the oral cavity, pharinx and larynx remain a significant public health problem. They represent 2-3% of all malignancies, and their incidence, particularly that of oral SCCs (OSCCs), is increasing in Western countries.[1] In spite of improved therapeutic procedures, the prognosis of OSCC patients is still poor and considerably lower than that of other neoplasias.[2] This fact can be attributed to several factors: failure to respond to available chemotherapy, late presentation of the lesions, and lack of suitable markers for early detection and prognosis.[3,4] Hence, the finding of novel tumour markers, particularly those associated with tumour cell invasion and spreading, can help provide a more accurate evaluation of prognosis and a more efficient management of the disease.

PA2.26 antigen was identified in our laboratory as a cell-surface protein induced in murine epidermal keratinocytes and dermal fibroblast-like cells during wound healing and chemical carcinogenesis.[5] Sequence analysis of the isolated cDNA and biochemical characterization of the protein revealed that murine PA2.26 is a small mucin-like transmembrane glycoprotein of about 45-kDa,[6] highly homologous to the rat alveolar type I cell marker T1α and the podocyte-associated glycoprotein podoplanin.[7,8] Murine PA2.26 nucleotide sequence is almost identical to that of OTS-8 and gp38, markers of the osteoblastic cell lineage and stromal cells in peripheral lymphoid tissues, respectively,[9,10] and completely matches the nucleotide sequence of RANDAM-2, a recently discovered membrane glycoprotein expressed in neuronal cells during mouse neurogenesis.[11] Expression of PA2.26/T1α is developmentally regulated, and has also been detected in the choroid plexuses, ependyma, mesothelia, endothelia of lymphatic vessels and ciliary epithelia, located at the apical surface and microvillous projections.[6,12] Other homologues include the rat glycoproteins RT140 and E11,[13,14] the

canine receptor for the influenza C virus gp40 and its human homologue gp36,[15,16] and the platelet aggregation-inducing sialoglycoprotein Aggrus.[17] The generation of knock-out mice containing a targeted mutation in the *T1α/PA2.26* gene locus has provided important insights concerning the involvement of this glycoprotein in normal tissue development. *T1α* null mice die at birth due to respiratory failure caused by anomalies in the development of alveoli.[18] These mice also showed defects in lymphatic, but not blood vessel pattern formation, associated with lymphedema, dilation of lymphatic vessels and diminished lymphatic transport.[19] Although the precise function of T1α/podoplanin/PA2.26 in normal tissues is still unknown, *T1α* null mouse defects have been attributed to disruption of epithelial-mesenchymal signalling[18] and to impaired cell to substratum adhesion and migration.[19]

Our previous studies suggested that induction of PA2.26 in mouse epidermal cells and tumours was related to cell migration and malignant progression.[6,20] For this reason, we focused on characterizing the human homologue of mouse PA2.26, and on studying its involvement in human cancer. In the present work, we report the molecular characterization of human PA2.26. Both mouse and human PA2.26 exhibit similar structural and biochemical characteristics and, likely, share the same function. We show that PA2.26 is induced in a subset of human early OSCCs, associated with downregulation of membrane E-cadherin protein expression. Furthermore, PA2.26 promotes the formation of cell-surface extensions and diminishes cell-cell adhesiveness when expressed in cultured human keratinocytes. These results suggest that PA2.26 might play an important role in tumour progression in human oral cancer.

Materials and Methods

Molecular characterization of PA2.26 cDNA

Mouse PA2.26 sequence was tested for similarity to known sequences deposited in the GenBank database using BLAST software.[21] Four overlapping IMAGE cDNA clones: 41487, 154633, 881369 and 1031768 containing a cDNA sequence highly homologous to that of mouse PA2.26 were purchased from the Medical Research Council Center (Cambridge, UK, Human Genome Mapping Project) and sequenced with an ABI PRISM 377 machine (PE Applied Biosystems, Foster City, CA). A CpG rich region extending from exon 1 to intron 1 was predicted by the GRAIL/cpg program at the Human Genome Mapping Project (http://menu.hgmp.mrc.ac.uk/menu-bin/Nix/Nix.pl). The chromosomal localization of the gene was performed by using the BLASTN and TBLASTN programs against the human genome (National Cancer for Biotechnology Information, NCBI). PA2.26 sequence was assigned to the NT_004577 contig localized at 1p36.13.

Plasmid construction

A partial human PA2.26 cDNA containing the full coding region was amplified from a human placenta cDNA library (Clontech Laboratories Inc. Palo Alto, CA) using the following oligonucleotides: 5'-CGGGATCGATGTGGAAGGTGTCAGC-3' and 5'-CCGCTCGAGGGCCACAGAAGTCAGAAACG-3' (nucleotides 196-763 of the sequence reported in Fig. 1*a*). PCR conditions were 30 cycles: 95ºC for 1 minute, 59ºC for 1 minute and 72ºC for 1 minute. The resulting 568-bp cDNA fragment was cloned into the pGEM-T Easy vector (Promega Corporation, Madison, WI, USA), sequenced in

both directions, and subcloned into the pcDNA3 expression vector ((InVitrogen, San Diego, CA).

To express human PA2.26 fused to the N-terminal end of the enhanced green fluorescent protein (PA2.26-GFP), the PA2.26 cDNA fragment containing the full coding region was amplified by PCR using oligonucleotides: 5'-GTGCTGGAATTCCCCGATGTGG-3' and 5'-TCAGGTACCCTGGGCGAGTACCTTCC-3', that introduce an EcoRI site (GAATTC) at the 5' end before codon 1 and a KpnI site (GGTACC) at the 3' end, after codon 162, eliminating the stop codon. The product was subcloned into the pEGFP-N1 expression vector (Clontech). Sequencing confirmed the correct ligation of the PA2.26 cDNA fragment.

Northern blot analysis

Commercial Northern blots containing poly(A)$^+$ RNA from adult human tissues (Clontech) were probed with PA2.26 and β-actin cDNAs according to the manufacturer's instructions. The probe for PA2.26 was a fragment of 568-bp cloned from placenta (see above).

Production of antibody

A polyclonal Ab against human PA2.26 was raised in a rabbit by immunization with the synthetic peptide Leu-Glu-Gly-Gly-Val-Ala-Met-Pro-Gly-Ala-Glu-Asp-Asp-Val-Val, comprising amino acids 37-51 of the protein ectodomain (P_{37-51}), coupled to keyhole limpet hemocyanin (Isogen Bioscience BV, Maarssen, The Netherlands). A subcutaneous injection of 500 μg of P_{37-51} (333 μg of the protein carrier) in complete Freund's adyuvant was given at multiple sites in the back of the animal, followed by

two booster injections in incomplete adyuvant at two-weeks and two-months intervals. The antiserum was concentrated by ammonium sulfate precipitation (50% saturation) and dialyzed against PBS/sodium azide. IgGs were purified by affinity chromatography through protein A-Sepharose 4B (Sigma-Aldrich, Madrid, Spain).

In vitro transcription/translation reaction

The PA2.26 cDNA subcloned into the pcDNA3 vector was *in vitro* transcribed and translated in the TNT-coupled wheat germ or rabbit reticulocyte extract systems (Promega) according to the manufacturer's instructions. The products of the reaction were fractioned on 12% SDS-PAGE gels and PA2.26 detected by Western blotting.

cDNA transfection and cell culture conditions

HeLa and HaCaT cell lines were grown in Dulbecco's modified Eagle's medium (DMEM) supplemented with 10% fetal calf serum (Gibco Invitrogen Corp., Barcelona, Spain) and antibiotics (25 μg/ml amphotericin B, 100 μg/ml ampicillin, and 32 μg/ml gentamicin; Sigma-Aldrich, Madrid, Spain). Cultures were maintained on plastic plates at 37ºC in a 5% CO_2 humidified atmosphere. HaCaT keratinocytes (passage 33) were kindly provided by Dr. Norbert E. Fusenig (German Cancer Research Center, Heidelberg, Germany). HeLa cells were obtained from the American Type Culture Collection (Rockville, MD, USA).

For transient transfections, cells were seeded on glass coverslips 24 h before DNA transfer, and then transfected with the PA2.26 cDNA subcloned into the pcDNA3 vector, using Effectene Transfection Reagent (Quiagen, Valencia, CA, USA). Immunofluorescence analysis was done 24 hours after transfection.

For stable transfections, cells cultured on plates were transfected with the PA2.26-EGFP construct or the empty pEGFP-N1 vector, as above. Transfected cells were selected by growing in DMEM containing 10% fetal calf serum and 0.5 mg/ml of G418 for 3-weeks. Individual clones were isolated with cloning rings, and characterized for PA2.26 expression by flow cytometry analysis and Western blotting.

Western blot analysis and glycosidase digestion

For detection of PA2.26 in Western blots, cells or tissues (obtained from the "Hospital Universitario de la Princesa", Madrid, Spain) were lysed in buffer RIPA (0.1% SDS, 0.5% sodium deoxycholate, 1% Nonidet P-40, 150 mM NaCl, 50 mM Tris-HCl, pH 8.0), and a cocktail of protease inhibitors (1 mM phenylmethylsulfonyl fluoride, 2 μg/ml aprotinin and 2 μg/ml leupeptin). Samples containing the same amount of protein (30 μg) were run on 10% or 7% SDS-PAGE and transferred to Immobilon P membranes (Millipore Corporation, Bedford, MA). Filters were immunoblotted with the PA2.26 Ab (at a dilution of 1:400 in PBS containing 1 mg/ml BSA) or preimmune serum at an equivalent dilution. As an additional control, the Ab was preincubated with an excess of either P_{37-51} (3 μg/ml) or an unrelated peptide (Gly-Ala-Ser-Lys-Cys-Asp-Gly-Phe-Arg-Ser, $P_{control}$) for 30 minutes. As secondary Ab, anti-rabbit IgG coupled to horseradish peroxidase (Nordic Immunological Laboratories, Tilburg, The Netherlands) was used. For detection of E-cadherin and α-tubulin in Western blots, the mAbs ECCD-2 and DM1A (Sigma Aldrich) were used at 1:100 and 1:10000 dilution, respectively. Peroxidase activity was detected using an enhanced chemiluminescence kit (ECL, Amersham Corporation, Arlington Heights, FL).

PA2.26 digestion with glycosidases was performed as previously described [6] in whole cell lysates (in buffer RIPA) obtained from HeLa cell transfectants, followed by Western blotting using the PA2.26 polyclonal Ab.

Immunohistochemistry

Paraffin-embedded sections of OSCCs and premalignant lesions were obtained from the archive of the Department of Clinical Pathology at the "Hospital Universitario de la Princesa" (Madrid, Spain). OSCC patients did not receive any therapeutic treatment prior to local resection surgery. All cases were confirmed to have negative lymphatic nodes by histology and were therefore classified as intraoral-confined disease. Clinical follow-up data were retrieved from the oral carcinoma database of the Department of Oral and Maxillofacial Surgery, Hospital Universitario de la Princesa. The minimum follow-up period was 3 years. The mean follow-up was 5 years.

PA2.26 immunostaining was performed directly in deparaffinized sections by either the Envision plus peroxidase method or the Labelled streptavidin-biotin (LSAB) 2 system, alkaline phosphatase (Dako Cytomation Inc., Glostrup, Denmark) or the avidin-biotin alkaline phosphatase method. The Ab was used at 1:400 dilution before and after preincubation with $P_{37\text{-}51}$ and $P_{control}$ peptides. Sections were dehydrated in graded ethanols, cleared in xylene, and mounted in Permount after counterstaining with hematoxylin and eosin. In all cases recorded as positive for PA2.26 immunostaining, labeling was proved to be blocked by preincubation of the Ab with $P_{37\text{-}51}$. E-cadherin immunostaining in tumour sections was performed by heat-induced antigen retrieval in a press cooker with EDTA solution, pH 8.0, for 2 min, using mAb 4A2C7 at 1:500 (Zymed Laboratories Inc., San Francisco, CA).

Confocal immunofluorescence microscopy analysis

Double immunofluorescence detection of PA2.26 and ezrin in HaCaT and HeLa cells transiently transfected with PA2.26 cDNA was performed on cells fixed with 3.7% formaldehyde in PBS, permeabilized with 0.05% Triton X-100. PA2.26 polyclonal Ab (before and after preincubation with $P_{37\text{-}51}$ and $P_{control}$ peptides, see above) and anti-ezrin mAb 3C12 (Sigma-Aldrich) were used at 1:100 dilution. FITC-labeled anti-rabbit or TRITC-labeled anti-mouse IgGs (Jackson, West Grove, PA) were used as secondary antibodies, respectively. For F-actin staining, phalloidin coupled to Rhodamin was used. Staining of nuclei was performed in a solution of 4', 6-diamino-2-phenilindole (DAPI, 1 μg/ml).

Immunofluorescence detection of E-cadherin and β-catenin in PA2.26-EGFP stable transfectants was carried out on confluent cells grown on glass coverslips, fixed in cold methanol,[22] using the mAbs 4A2C7 (Zymed Laboratories Inc.) and C19220 (Transduction Laboratories, Lexington, KY) at 1:100 and 1:250 dilutions, respectively, and appropriate TRITC-labeled secondary Abs.

Double-label immunofluorescence detection of PA2.26 and ezrin or E-cadherin in tumour sections was performed after heat-induced antigen retrieval and proteinase K digestion for 10 minutes at 37ºC. Sections were blocked in PBS containing 1% BSA and incubated with PA2.26 Ab and anti-ezrin 3C12 or anti-E-cadherin 4A2C7 mAbs. Alexa Fluor 588 goat anti-rabbit IgG or Alexa Fluor 594 goat anti-mouse IgG (Molecular Probes Europe BV, Leiden, The Netherlands) were used as secondary Abs. Tissue sections were then mounted in Mowiol and examined with a confocal microscope.

Confocal laser scanning microscopy was performed with a Leica TCS-SP2 (Leica Lassertechnik GmbH, Heidelberg, Germany) adapted to an inverted Leitz DMIRB

microscope. Images were taken using a 63X (NA 1.4 oil) Leitz Plan-Apochromatic objective. 10-25 optical sections of 0.3 μm were made for three-dimensional reconstruction through the whole depth of the cells, and projections of 5-6 sections were used for reconstruction of particular cellular domains. For tissue samples, 12 optical sections of 0.5 μm were made. Images were assembled using Leica confocal software 2.0.

Cell aggregation assay

Ca^{2+}-dependent cell aggregation assays were performed according to Navarro and coworkers.[22] Briefly, cell cultures were dissociated into single-cell suspensions under E-cadherin-saving conditions. Cells were suspended in 10 mM Hepes, pH 7.4, 150 mM NaCl containing 0.5% BSA and 10 mM $CaCl_2$ or 1 mM EGTA, and incubated under gyratory shaking at 80 rpm for 60 minutes. The degree of cell aggregation was expressed by the aggregation index: $1-(N_{60}/N_0)$, where N_0 and N_{60} indicate the initial number of particles and the number of particles after 60 minutes of aggregation, respectively. All N_0 and N_{60} measurements were done in duplicates, and the experiments were repeated at least twice.

Results

cDNA cloning, exon/intron organization, and chromosomal mapping

Several ESTs with significant homology to the mouse *PA2.26* mRNA[6] were identified by database comparison. Four overlapping IMAGE clones containing the full-length cDNA were acquired from the Medical Research Council Center (Cambridge, UK, Human Genome Mapping Project) and their sequences determined. The 2737-nt cDNA obtained (Fig. 1*a*) contains a single polyadenylation consensus sequence

AATAAA and an open reading frame (ORF) encoding a 162 amino acid protein highly homologous to the 172-amino acid mouse PA2.26 protein. The human PA2.26 protein exhibits the typical structure of a type-I membrane mucin-like protein with an ectodomain containing a high proportion of potential O-glycosylation serine and threonine residues, and a presumptive spanning membrane domain followed by a short cytoplasmic tail of 9 amino acids (Fig. 1*a* and *b*). The cytoplasmic domain of the human protein conserves a cluster of three basic aminoacids (Fig. 1*b*) shared by transmembrane proteins of microvillal location[23] that appears to be responsible for PA2.26 binding to proteins of the ezrin, radixin, moesin (ERM) family.[6]

Database comparison of the complete 2737-nt cDNA sequence presented in Fig. 1*a* revealed the presence of several ESTs belonging to the same transcriptional unit, further extending the 5' UTR end by 8 nt (Access to GenBank BE563074/AA301065), by 37 nt (AU133042), and by 114 nt (BE887331), indicating the possible existence of other transcription initiation sites. Thus, a larger cDNA sequence registered in the GenBank (under accession number NP-006465) contains an alternative ATG start codon 5' upstream of the sequence presented in Fig. 1*a*, predicting a new ORF, which includes de coding sequence reported here plus additional 76 N-terminal amino acids. We believe that this larger, alternative, polypeptide is unlikely to be expressed in human tissues because it lacks a signal peptide in the amino terminus for protein delivery to the plasma membrane, which is conserved in the mouse, rat and canine homologues.[6,7,15] In addition, we show in this work that the size of the protein expressed by our cloned cDNA after transfection into mammalian cells coincides with that of the endogenous PA2.26 protein detected in human tissues by Western blotting (see below). The ORF encoding human PA2.26 is identical to that described for *gp36* and *T1α-2*, the human homologues of canine *gp40* and rat *T1α*, respectively.[16,24] However, the reported *gp36*

and *T1α-2* cDNA sequences are incomplete (768 and 865-bp, respectively) and have many changes in UTRs with respect to the *PA2.26* sequence reported here. In addition, a 1013-bp cDNA sequence for human *podoplanin* has been delivered to GenBank (under accession number AF390106). This sequence is identical to that reported here for *PA2.26* and corresponds to positions 21 to 1033 of the cDNA sequence showed in Fig. 1*a*.

Alignment of the *PA2.26* cDNA sequence with human genomic sequences deposited in GenBank predicts that the human *PA2.26* gene contains 6 exons and 5 introns. The lengths of introns and exons are shown in Fig.1*c*. All the intron-exon junctions follow the canonical AG-GT rules. The first exon contains the initiation codon ATG and a 5' UTR of 203-nt. The last exon contains the termination codon followed by a 1769-nt UTR which includes a 200-nt AluSc sequence in the reverse orientation at the 3' end (Fig. 1*a*). The largest intron (> 22.746 nt) lies between exons 1 and 2. A 432-nt CpG island was predicted that comprises the last 182 nt of the exon 1 and the first 250 nt of intron 1. We could assign the *PA2.26* sequence to the NT_004577 contig localized to the short arm of chromosome 1 at 1p36.13.

Expression studies in normal tissues

Northern blot analysis with RNA isolated from various adult human tissues using a PA2.26 probe containing the full coding sequence amplified from a placenta cDNA library (see Materials and Methods), revealed two mRNA species of about 2.7-kb and 0.9-kb (Fig. 2). The larger transcript corresponds to the estimated size of the full-length human *PA2.26* cDNA presented in Fig. 1*a*. The origin of the 0.9-kb message is unknown at the present time. Clear expression of PA2.26 transcripts was observed in skeletal muscle, placenta and heart, and, at a lower level, in lung. The 2.7-kb transcript

was the most abundant of the two transcripts in the majority of these tissues. No specific signal could be detected in several other tissues, such as brain, liver, kidney and pancreas, even after long exposure of the autoradiography.

Production of a specific polyclonal antibody

Since our previous mAb generated against the mouse PA2.26 antigen[6] was found not to recognize the human protein, we synthesized a peptide comprising amino acids 37-51 (P_{37-51}) of the extracellular domain of human PA2.26, a region that does not contain glycosylation residues. This peptide was used to immunize rabbits (see Materials and Methods). To test whether the obtained polyclonal Ab recognized PA2.26, we synthesized the protein encoded by the *PA2.26* cDNA by a coupled transcription/translation reaction using a cell-free wheat germ extract system. A polypeptide of about 21-kDa corresponding to the core protein of PA2.26 was synthesized, as detected in a Western blot (Fig. 3*a*). Preincubation of the Ab with P_{37-51}, but not with an unrelated peptide ($P_{control}$), prevented recognition of the 21-kDa polypeptide, indicating that the Ab was specific for the P_{37-51} amino acid sequence of PA2.26. The same result was obtained using a rabbit reticulocyte extract system to transcribe/translate the gene (data not shown). To test whether the Ab recognized the PA2.26 protein expressed in mammalian cells, PA2.26 cDNA was transfected into HeLa cells, which do not express endogenous PA2.26. As shown in Fig. 3*b*, the Ab specifically recognized a protein of about 38-40 kDa, which corresponds to the glycosylated mature form of PA2.26, as demonstrated by treatment with glycosidases (not shown). PA2.26 was neither expressed in parental HeLa cells nor in cells transfected with the empty vector. The Ab recognized a polypeptide of the expected size, 61 kDa, corresponding to PA2.26 expressed as a C-terminal fusion protein with

EGFP (PA2.26-EGFP, see Fig. 3*d*). To confirm the O-glycosylation of human PA2.26 in the fusion protein, cell lysates were digested with glycosidases, followed by Western blotting with the PA2.26 Ab. Sequential digestion with neuraminidase and O-glycosidase yielded a molecular mass reduction of about 11 kDa, while treatment with O-glycosidase alone did not affect the mobility of the protein (Fig. 3*d*), indicating that human PA2.26 protein is heavily O-glycosylated and contains sialic acid, just as the mouse PA2.26 protein.[6] We also studied whether the Ab recognized the native PA2.26 protein expressed in human tissues. As shown in Fig. 3*c*, protein forms of the same size as that of the exogenous PA2.26 protein expressed in HeLa cell transfectants were detected in placenta, lung and testis lysates by Western blotting, indicating that the protein encoded by the cloned cDNA has the same molecular mass than the endogenous PA2.26 protein. The level of PA2.26 protein expression in lung was lower compared with placenta and testis, which is in agreement with the Northern blot data (see Fig. 2). Testis (which was not screened for PA2.26 expression by Northern blot hybridization) was used in this assay because it proved to be positive for PA2.26 expression by immunohistochemistry (not shown).

PA2.26 is expressed in oral squamous cell carcinomas

Since a preliminary RT-PCR analysis showed PA2.26 mRNA expression in some human OSCC cell lines (data not shown), we studied the expression of PA2.26 in primary oral tumours by immunohistochemistry. We found that PA2.26 is induced in about 25% (15 out of 61 cases) of early OSCCs located at floor of mouth and tongue (Table 1). A small number (n = 6) of gingival SCCs were also screened and found not to express PA2.26 (data not shown). No significant correlation was observed between PA2.26 expression and tumour differentiation grade (Table 1). No association was

found, either, between PA2.26 expression and clinical parameters, such as the age of patients, sex, survival and locoregional recurrence. For instance, the average age of patients included in the PA2.26-positive group was 52.00 $\pm$ 10.39 (12 males and 3 females) compared with 56.23 $\pm$ 11.49 (38 males and 8 females) in the PA2.26-negative group. During the follow-up period (3 years minimum), the recurrence rate in the PA2.26-positive group was of 20% (3 out of 15), while the mortality rate due to tumour-related causes was of 7% (1 out of 15), compared with 20% (9 out of 46) of patients who showed local or regional recurrences and 9% (4 out of 46) of patients dead in the PA2.26-negative group.

PA2.26 expression in OSCCs was heterogeneous, often restricted to the growth front of the tumours (Fig. 4*e*), and was predominantly located at the plasma membrane (Fig. 4*g*). PA2.26 was neither detected in the normal oral epithelium (Fig. 4*a*), nor in premalignant lesions (n = 10) exhibiting moderate to intense dysplasia (Fig. 4*b*). However, a positive staining was seen frequently in the reactive mucosa adjacent to OSCCs, including those lesions stained weakly or not stained at all with the PA2.26 Ab (Fig. 4*c* and *d*). PA2.26 expression in the hyperplastic mucosa was restricted to basal-like cells and no expression was seen in differentiating keratinocytes of suprabasal layers (Fig. 4*d*). Since mouse PA2.26 was found to destabilize E-cadherin-mediated cell to cell adhesions when expressed in keratinocytes[20], sections from PA2.26-positive tumours were also stained with an anti-E-cadherin mAb. We found that E-cadherin expression in the tumours was also very heterogenous, with some areas showing an intense staining and others in which E-cadherin staining was fragmented or virtually absent (Fig. 4*f*, *h*). Interestingly, some regions that expressed PA2.26 seemed to exclude the presence of E-cadherin (Fig. 4, compare panels *e* and *f*). In other cases, PA2.26 tended to be expressed in the layer of keratinocytes in contact with the stroma, while E-

cadherin staining was mainly suprabasal (Fig. 4, compare panels *g* and *h*). Because of the preferential expression of PA2.26 in the basal layer of hyperplastic mucosa and tumour nests, we analyzed whether the presence of PA2.26 was restricted to proliferative cells by immunohistochemical staining with Ki-67, but no clear correlation between expression of this proliferation nuclear marker and that of PA2.26 was found (data not shown).

The inverse correlation observed between PA2.26 and E-cadherin expression at the surface of carcinoma cells was further analyzed by double immunofluorescence and confocal microscopy studies in a representative number of PA2.26-positive SCCs of the tongue (n = 5). In all cases, E-cadherin protein was reduced or virtually absent at cell-cell contacts in tumour nests that expressed PA2.26 (Fig. 5*b-d*). Conversely, a normal pattern of E-cadherin staining at cell-cell junctions was observed in regions that were negative for PA2.26 staining (insets in Fig. 5*b-d*). In contrast, PA2.26 and ezrin focally colocalized *in vivo* at the plasma membrane of tumour cells (Fig. 5*f-h* and insets). These results suggest that expression of PA2.26 in OSCCs might be associated with destabilization of E-cadherin-mediated cell-cell adhesion.

PA2.26 induces cell-surface protrusions and reduces cell-cell adhesiveness

To analyze the effects of PA2.26 expression on the phenotype of human epithelial cells, we transiently transfected HeLa carcinoma cells and HaCaT immortalized keratinocytes with the human PA2.26 cDNA, since these cell lines were previously found not to express PA2.26 mRNA by RT-PCR (data not shown). Immunofluorescence staining and confocal microscopy analysis showed that PA2.26 protein was directed to the cell surface (Fig. 6). Vertical optical sections indicated that PA2.26 was distributed in a clustered pattern all over the plasma membrane (Fig. 6*c* and

d), suggesting that the antigen was concentrated at cell-surface protrusions. This was confirmed with a three-dimensional reconstruction of the upper part of transfected cells (Figure 6*a* and *b*). We also studied by double immunofluorescence analysis whether human PA2.26 colocalized with ezrin at plasma membrane protrusions. Ezrin was located as a punctate staining distributed uniformly throughout (underneath) the plasma membrane in HeLa cells that did not express PA2.26 (Fig. 6*f* and *g*), in a pattern typical of microvilli.[25] However, in cells expressing PA2.26, ezrin was relocated to the cell edges where it colocalized with PA2.26 on membrane projections (Fig. 6*e-g*). A similar effect, although less pronounced, was observed in HaCaT cell transfectants (Fig. 6*h-j*). This milder effect could be due to the lower PA2.26 expression level at the cell surface obtained in this latter cell line. In contrast to HeLa, expression of PA2.26 in HaCaT keratinocytes was unstable, as suggested by the presence of many transfectant cells with endocytic vesicles containing PA2.26 (data not shown). Both the density and length of projections protruding from the cell edges appeared to be enhanced in transfected cells with respect to the non-transfected ones (Fig. 6*e-j*, arrows). Many of these PA2.26-containing projections had lengths of >5 μm (insets in Fig. 6*e-g*), and formed phalloidin-positive F-actin bundles at the periphery (not shown), resembling filopodia.[26,27] In contrast, in cells that did not express PA2.26, most of ezrin-positive cell-surface protrusions were microvilli or microspikes (<5 μm).

Since HeLa are not cohesive cells and have lost E-cadherin expression,[28,29] we studied the effect of PA2.26 on cell-cell adhesiveness in HaCaT keratinocytes. To this aim, HaCaT cells were stably transfected with a vector encoding PA2.26 fused to EGFP (PA2.26-EGFP). This procedure resulted in a more stable expression of PA2.26 at the cell surface when compared to the above transfection experiment. PA2.26-EGFP was also directed to cell-surface projections (Fig. 7*f*), where it colocalized with ezrin and F-

actin (not shown), while EGFP was distributed uniformly throughout the cytoplasm in control cells transfected with the empty vector (inset in Fig. 7*b*). Control transfectants grown at confluence showed the typical tight cell-cell contacts of keratinocytes (Fig. 7*a*), decorated by a continuous line of E-cadherin and β-catenin staining (Fig. 7*c* and *d*). In contrast, aberrant cell-cell borders with irregular outlines (Fig. 7*e*), and intercellular spaces filled with PA2.26-containing microvilli (Fig.7*f* and inset), were observed in PA2.26-EGFP transfectants. These cells showed a rather disorganized pattern of E-cadherin and β-catenin distribution, characterized by the presence of both proteins out of cell-cell contacts (Fig. 7*g*-*h* and insets).

To ascertain whether expression of PA2.26 in HaCaT keratinocytes impaired E-cadherin function, a Ca^{2+}-dependent cell aggregation assay was performed in selected clones expressing varying amounts of PA2.26-EGFP (Fig. 8). Ca^{2+}-dependent cell-cell adhesiveness decreased in PA2.26-EGFP transfectants in comparison with the parental cell line or control cells (Fig 8*b* and *c*), in direct proportion to the level of PA2.26-EGFP expression (Fig 8*a*). Although a slight reduction of E-cadherin protein levels was found in PA2.26-EGFP transfectants with respect to control cells, it did not correlate with the level of PA2.26-EGFP expression (Fig. 8*a*), suggesting that PA2.26 reduces HaCaT cell-cell adhesiveness by a mechanism that does not necessarily involve downregulation of E-cadherin expression.

Discussion

We report in this article the full cDNA sequence of the human homologue of murine PA2.26 antigen. The human *PA2.26* gene is expressed as two mRNAs of 2.7- and 0.9-kb in the placenta, heart, skeletal muscle and lung. These two transcripts have also been reported for podoplanin in human lymphatic endothelial cells.[30] The size of

the larger mRNA detected in human tissues by Northern blot hybridization fits the length of the cDNA reported here for PA2.26. It encodes a small mucin-type transmembrane glycoprotein of 162 amino acids practically identical to T1α-2, gp36 and podoplanin[16,24], which is detected as a 38-40-kDa protein form in transfected cells and human tissue lysates in Western blots, using a polyclonal Ab raised against a peptide of the ectodomain. Nevertheless, the presence of an alternative mRNA of 0.9-kb in human tissues might suggest the existence of other protein isoforms not detected by this Ab.

The main finding of this study is that expression of PA2.26 (T1α, podoplanin) is induced in a subset of human early OSCCs. This observation strengthens our previous work showing the induction of PA2.26 during mouse skin carcinogenesis related to cell migration and invasion/metastasis. [5,6,20] Both, oral and skin carcinogenesis are multistep processes in which multiple genetic events lead to the disruption of normal regulatory pathways controlling cell division, differentiation and cell death.[31,32] SCCs are characterized by their ability to spread locally and regionally, and tumour infiltration involves, among other factors, alterations in the expression and/or function of cell adhesion molecules, such as E-cadherin.[33,34] Reduced expression of E-cadherin and β-catenin at the plasma membrane have been found in OSCCs associated with the degree of tumour differentiation and poor prognosis.[34-37] Thus, expression of E-cadherin is homogeneously reduced at late stages in poorly differentiated carcinomas, apparently by a mechanism that involves hypermethylation of the gene promoter.[38-40] However, well and moderately differentiated OSCCs often show a partial loss of membrane E-cadherin and β-catenin expression, circumscribed to some tumour regions or even to certain areas of tumour nests.[34,35] PA2.26 expression in early OSCCs is heterogeneous and fragmented, frequently restricted to the invasive tumour front, and correlates with

reduced membrane E-cadherin expression *in vivo* and with impaired cell-cell adhesiveness *in vitro*. These results suggest that the presence of PA2.26 in OSCCs can be related to a migratory/invasive phenotype.

The effect of PA2.26 on cell-cell adhesiveness appears to be indirect, involving the reorganization of the actin cytoskeleton by recruitment of ezrin and the induction of cell-surface protrusions. The ERM proteins have been implicated in the organization of specialized membrane domains, and in the control of cell shape, cell adhesion and migration, by linking transmembrane proteins to the actin cytoskeleton.[25,41] Mouse PA2.26 was shown to coimmunoprecipitate with ezrin and moesin,[6] and a yuxtamembrane cluster of basic amino acids which appears to be responsible for murine PA2.26 binding to ERM proteins is conserved in the human PA2.26 endodomain. In fact, human PA2.26 colocalizes with ezrin *in vivo* at the surface of oral carcinoma cells and at membrane projections of HeLa and HaCaT cell transfectants. It is likely that PA2.26-induced redistribution of ezrin and formation of cell-surface extensions disrupt the anchorage of E-cadherin-catenin complexes to the cortical actin cytoskeleton. Interestingly, Pujuguet and coworkers show in a recent report that a constitutively active mutant form of ezrin, when expressed in cultured epithelial cells, causes extensive lamellipodia formation and disturbs E-cadherin-dependent cell-cell contacts via activation of Rac1, but not of other Rho GTPases.[42] These results suggest a role of ezrin in cell-cell junction assembly. Whether the effects of PA2.26 on the cell membrane and cytoskeleton involve changes in the activity of Rho GTPases is currently being investigated. Ectopic expression of mouse PA2.26 in premalignant murine keratinocytes (MCA3D cell line) elicited a complete epithelial-mesenchymal transition, with loss of E-cadherin protein (but not mRNA) expression, and acquisition of a fibroblast-like morphology associated with development of undifferentiated carcinomas.[6,20] In contrast,

human PA2.26 expressed in immortal HaCaT keratinocytes failed to trigger a complete epithelial-mesenchymal transition, but induced cell scattering associated with increased plasma membrane motility and reduced cell-cell cohesion. To explain this apparent discrepancy, it should be noted that HaCaT keratinocytes are nontumorigenic when injected subcutaneously or grafted as surface transplants onto nude mice, and, therefore, represent a preneoplastic stage of tumour development[43]. MCA3D keratinocytes, on the other hand, can develop tumours in skin graft experiments and are considered a premalignant cell line,[20] a step further in tumour progression compared with HaCaT cells. Consequently, it is likely that PA2.26 needs to cooperate with other genetic or epigenetic events to confer a full malignant phenotype in keratinocytes.

Similar effects on the plasma membrane and cell-cell adhesiveness have been recently found for dysadherin, a different mucin-type glycoprotein of 178 amino acids, also associated with cancer. Transfection of dysadherin cDNA into liver cancer cells resulted in formation of numerous microvilli and impaired cell-cell adhesiveness without affecting E-cadherin mRNA expression.[44] In contrast with other known cancer anti-adhesive mucins of very large molecular masses (> 200 kDa), such as MUC1 (episialin) and MUC4 (sialomucin),[45,46] PA2.26 and dysadherin belong to a group of cancer membrane mucins characterized by their relatively small size. Both PA2.26 and dysadherin appear to downregulate E-cadherin function in carcinoma cells by a novel mechanism involving a reorganization of the actin cytoskeleton.

Acknowledgements

We thank Norbert E. Fusenig for his generous gift of HaCaT keratinocytes. We also thank Diego Megías for helping us with confocal microscopy; Monica García-Gallo, Eva MG Marazuela and Cristina González for skilful technical assistance; David

Sarrió for helpful suggestions and Jaime Renart for critical reading of the manuscript. This work was supported by grants from the "Fondo de Investigaciones Sanitarias" (FIS-01/1125 to M.Q. and FIS-02/1025 to C.G.) and the "Ministerio de Ciencia y Tecnología" (SAF2001-2361). E.M-V. was the recipient of a predoctoral fellowship from the FIS. M.M.Y. was funded by a predoctoral fellowship from the "Fundación Carolina".

References

1. Parkin DM, Pisani P, Ferlay J. Global cancer statistics. CA Cancer J Clin 1999;49: 36-64.

2. Neville BV, Day TA. Oral cancer and precancerous lesions. CA Cancer J Clin 2002;52:195-215.

3. Patel V, Leethanakul C, Gutkind JS. New approaches to the understanding of the molecular basis of oral cancer. Crit Rev Oral Biol Med 2001;12:55-63.

4. Nagler RM. Molecular aspects of oral cancer. Anticancer Res 2002;22:2977-2980.

5. Gandarillas A, Scholl FG, Benito N, Gamallo C, Quintanilla M. Induction of PA2.26, a cell-surface antigen expressed by active fibroblasts, in mouse epidermal keratinocytes during carcinogenesis. Mol Carcinog 1997;20:10-18.

6. Scholl FG, Gamallo C, Vilaró S, Quintanilla M. Identification of PA2.26 antigen as a novel cell-surface mucin-type glycoprotein that induces plasma membrane extensions and increased motility in keratinocytes. J Cell Sci 1999;112:4601-4613.

7. Rishi AK, Joyce-Brady M, Fisher J, Dobbs LG, Floros J, Van der Spek J, Brody JS, Williams MC. Cloning, characterization, and developmental expression of a rat lung alveolar type I cell gene in embryonic endodermal and neural derivatives. Dev Biol 1995;167:294-306.

8. Breiteneder-Geleff S, Matsui K, Soleiman A, Meraner P, Poczewski H, Kalt R, Schaffner G, Kerjaschki D. Podoplanin, novel 43-kd membrane protein of glomerular epithelial cells, is down-regulated in puromycin nephrosis. Am J Pathol 1997;151:1141-1152.

9. Nose K, Saito H, Kuroki T. Isolation of a gene sequence induced later by tumor-promoting 12-O-tetradecanoylphorbol-13-acetate in mouse osteoblastic cells (MC3T3-E1) and expressed constitutively in ras-transformed cells. Cell Growth Differ 1990;1:511-518.

10. Farr AG, Berry ML, Kim A, Nelson AJ, Welch MP, Aruffo A. Characterization and cloning of a novel glycoprotein expressed by stromal cells in T-dependent areas of peripheral lymphoid tissues. J Exp Med 1992; 176:1477-1482.

11. Kotani M, Tajima Y, Osanai T, Irie A, Iwatsuki K, Kanai-Azuma M, Imada M, Kato H, Shitara H, Kubo H, Sakuraba H. Complementary DNA cloning and characterization of RANDAM-2, a type I membrane molecule specifically expressed on glutamatergic neuronal cells in the mouse cerebrum. J Neurosci Res 2003; 73:603-613.

12. Williams MC, Cao YX, Hinds A, Rishi AK, Wetterwald A. T1α protein is developmentally regulated and expressed by alveolar type I cells, choroids plexus, and ciliary epithelia of adult rats. Am J Respir Cell Mol Biol 1996;14:577-585.

13. Gonzalez RF, Dobbs IG. Purification and analysis of RT140, a type I alveolar epithelial cell apical membrane protein. Biochim Biophys Acta 1998;1429:208-216.

14. Wetterwald A, Hoffstetter W, Cecchini MG, Lanske B, Wagner C, Fleish H, Atkinson M Characterization and cloning of the E11 antigen, a marker expressed by rat osteoblasts and osteocytes. Bone 1996;18:125-132.

15. Zimmer G, Lottspeich F, Maisner A, Klenk HD, Herrler G. Molecular characterization of gp40, a mucin-type glycoprotein from the apical plasma membrane of Madin-Darby canine kidney cells (type I). Biochem J 1997;326:99-108.

16. Zimmer G, Oefner F, von Messling V, Tschernig T, Gröne H-J, Klenk H-D, Herrler G. Cloning and characterization of gp36, a human mucin-type glycoprotein preferentially expressed in vascular endothelium. Biochem J 1999;341:277-284.

17. Kato Y, Fujita N, Kunita A, Sato S, Kaneko M, Osawa M, Tsuruo T. Molecular identification of Aggrus/T1α as a platelet aggregation-inducing factor expressed in colorectal tumors. J Biol Chem 2003;278:51599-51605.

18. Ramirez MI, Millien G, Hinds A, Cao YX, Selding DC, Williams MC. T1α, a lung type I cell differentiation gene, is required for normal lung cell proliferation and alveolus formation at birth. Dev Biol 2003;256:61-72.

19. Schacht V, Ramirez MI, Hong Y-K, Hirakawa S, Feng D, Harvey N, Williams M, Dvorak AM, Dvorak HF, Oliver G, Detmar M. T1α/podoplanin deficiency disrupts normal lymphatic vasculature formation and causes lymphedema. EMBO J 2003;22:3546-3556.

20. Scholl FG, Gamallo C, Quintanilla M. Ectopic expression of PA2.26 antigen in epidermal keratinocytes leads to destabilization of adherens junctions and malignant progression. Lab Invest 2000;80:1749-1759.

21. Altschul SF, Madden TL, Schaffer AA, Zhang J, Zhang Z, Miller W, Lipman DJ. Gapped BLAST and PSI-BLAST: A new generation of protein database search programs. Nucleic Acids Res 1997;25:3389-3402.

22. Navarro P, Lozano E, Cano A. Expression of E- or P-cadherin is not sufficient to modify the morphology and the tumorigenic behavior of murine spindle carcinoma cells. Possible involvement of plakoglobin. J Cell Sci 1993;105;923-934.

23. Yonemura S, Hirao M, Doi Y, Takahashi N, Kondo T, Tsukita Sa, Tsukita Sh. Ezrin/radixin/moesin (ERM)-binding proteins bind to a positively charged amino acid cluster in the yuxta-membrane cytoplasmic domain of CD44, CD43, and ICAM-2. J Cell Biol 1998;140:885-895.

24. Ma T, Yang B, Matthay MA, Verkman AS. Evidence against a role of mouse, rat, and two cloned human T1α isoforms as a water channel or a regulator of aquoporin-type water channels. Am J Respir Cell Mol Biol 1998;19:143-149.

25. Bretscher A, Edwards K, Fehon RG. ERM proteins and merlin: integrators at cell cortex. Nat Rev Mol Cell Biol 2002;8:586-599.

26. Mitchison TJ, Cramer LP. Actin-based cell motility and cell locomotion. Cell 1996;84:371-379.

27. Small JV, Stradal T, Vignal E, Rottner K. The lamellipodium: where motility begins. Trends Cell Biol 2002;12:112-120.

28. Denk C, Hulsken J, Schwarz E. Reduced gene expression of E-cadherin and associated catenins in human cervical carcinoma cell lines. Cancer Lett 1997;120:185-193.

29. Chen CL, Liu SS, Ip SM, Wong LC, Ng TY, Ngan HY. E-cadherin expression is silenced by DNA methylation in cervical cancer cell lines and tumours. Eur J Cancer 2003;39:517-523.

30. Kriehuber E, Breiteneder-Geleff S, Groeger M, Soleiman A., Schoppmann SF, Stingl G, Kerjaschki D, Maurer D. Isolation and characterization of dermal lymphatic and blood endothelial cells reveal stable and functionally specialized cell lineages. J Exp Med 2001;194:797-808.

31. Yuspa SH. The pathogenesis of squamous cell cancer: Lessons learned from studies of skin carcinogenesis –Thirty-third GHA Clowes Memorial Award Lecture. Cancer Res 1994;54:1178-1189.

32. Williams HK. Molecular pathogenesis of oral squamous carcinoma. J Clin Pathol Mol Pathol 2000;53:165-172.

33. Cano A, Gamallo C, Kemp CJ, Benito N, Palacios J, Quintanilla M, Balmain A. Expression pattern of the cell adhesion molecules E-cadherin, P-cadherin and $\alpha_6\beta_4$ integrin is altered in pre-malignant skin tumors of p53-deficient mice. Int J Cancer 1996;65:254-262.

34. Bagutti C, Speight PM, Watt FM. Comparison of integrin, cadherin, and catenin expression in squamous cell carcinomas of the oral cavity. J Pathol 1998;186:8-16.

35. Lo Muzio L, Stalbano S, Pannone G, Grieco M, Mignogna MD, Cerrato A, Testa NF, De Rosa G. β- and γ-catenin expression in oral squamous cell carcinomas. Anticancer Res 1999;19:3817-3826.

36. Bankfalvi A, Krassort M, Vegh A, Felszeghy E, Piffko J. Deranged expression of E-cadherin/β -catenin complex and the epidermal growth factor receptor in the clinical evolution and progression of oral squamous cell carcinomas. J Oral Pathol Med 2002;31:450-457.

37. Tanaka N, Odajima T, Ogi K, Ikeda T, Satoh M. Expression of E-cadherin, α-catenin, and β-catenin in the process of lymph node metastasis in oral squamous cell carcinoma. Br J Cancer 2003;89:557-563.

38. Nakayama S, Sasaki A, Mese H, Alcalde RE, Tsuji T, Matsumura T. The E-cadherin gene is silenced by CpG methylation in human oral squamous cell carcinomas. Int J Cancer 2001;93:667-673.

39. Chang HW, Chow V, Lam KY, Wei WI, Yuen A. Loss of E-cadherin expression resulting from promoter hypermethylation in oral tongue carcinoma and its prognostic significance. Cancer 2002;94:386-392.

40. Viswanathan M, Tsuchida N, Shanmugam G. Promoter hypermethylation profile of tumor-associated genes p16, p15, hMLH1, MGMT and E-cadherin in oral squamous cell carcinoma. Int J Cancer 2003;20:41-46.

41. McClatchey AI. Merlin and ERM proteins: unappreciated roles in cancer development? Nat Rev Cancer 2003;3:877-883.

42. Pujuguet P, Del Maestro L, Gautreau A, Louvard D, Arpin M. Ezrín regulates E-cadherin-dependent adherens junction assembly through Rac1 activation. Mol Biol Cell 2003;14:2181-2191.

43. Fusenig NE, Boukamp P. Multiple stages and genetic alterations in immortalization, malignant transformation, and tumor progression of human skin keratinocytes. Mol Carcinog 1998;23:144-158.

44. Ino Y, Gotoh M, Sakamoto M, Tsukagoshi K, Hirohashi S. Dysadherin, a cancer-associated cell membrane glycoprotein, down-regulates E-cadherin and promotes metastasis. Proc Natl Acad Sci USA 2002;99:365-370.

45. Hilkens J, Marjolÿn J, Ligtenberg L, Vos HL, Litinov SV. Cell membrane-associated mucins and their adhesion-modulating properties. Trends Biochem Sci 1992;17:359-363.

46. Gendler SJ, Spicer AP. Epithelial mucin genes. Annu Rev Physiol 1995;57:607-634.

Legends to Figures

Figure 1. (*a*) Nucleotide sequence and predicted protein product of human PA2.26 cDNA. The vertical arrows indicate the exon-intron junctions. The N-terminal signal sequence is underlined and the membrane-spanning domain is shaded. Boldface amino acids represent the peptide sequence (P_{37-51}) used for immunization in order to raise a PA2.26 polyclonal Ab. A partial AluSc sequence at the 3' end is in boldface and italics. The highly conserved AATAAA polyadenylation signal sequence is indicated. The sequence is available from GenBank under accesion number AY194238. (*b*) Schematic representation of mouse and human PA2.26 protein domains. SP, signal peptide; ECTO, ectodomain; TM, transmembrane domain; ENDO, endodomain. Percentages indicate identical residues in the mouse and human polypeptides. A cluster of basic amino acids (underlined) potentially responsible for binding to ERM proteins and a potential protein kinase A/protein kinase C-dependent phosphorylation Ser (bolded) are conserved in the mouse and human PA2.26 endodomains. (*c*) Schematic representation of the PA2.26 exon-intron structure. Boxes represent exons and open boxes contain untranslated regions. The dotted zone indicates the position of the AluSc sequence. The sizes of exons and introns are indicated in bp and kb, respectively.

Figure 2. Analysis of PA2.26 mRNA expression in human tissues. Multi-tissue Northern blot hybridization revealed two mRNA bands of around 2.7-kb and 0.9-kb in size in skeletal muscle, placenta, heart and lung. A β-actin probe was used as a control for RNA quality and amount.

Figure 3. Characterization of the human PA2.26 cDNA product. (*a*) *In vitro* transcription/translation of PA2.26 cDNA using a TNT-coupled wheat germ extract system. The products of the reaction with and without (input) PA2.26 cDNA subcloned into the pcDNA3 vector were subjected to Western blot using PA2.26 Ab preincubated with $P_{37\text{-}51}$ or an unrelated peptide ($P_{control}$). (*b*) Specific detection of PA2.26 protein in HeLa cells transfected with PA2.26 cDNA by Western blot analysis as in panel *a*. Immunodetection of α-tubulin was used as a control for protein loading. (*c*) Comparison of molecular masses of exogenous PA2.26 protein expressed in HeLa cells and endogenous PA2.26 protein detected in human tissues by Western blotting. (*d*) Detection of PA2.26-EGFP in HeLa cells transfected with a PA2.26-EGFP fusion construct before and after treatment with neuraminidase (Na) and O-glycosidase (O-Gly) by Western blotting using PA2.26 Ab.

Figure 4. Immunohistochemical detection of PA2.26 in human OSCCs. (*a*) Normal oral epithelium. PA2.26 is absent from all epithelial layers (e) but present in lymphatic vessels (lv) and interstitial fibroblast-like cells (arrows) in the underlying connective tissue. (*b*) Carcinoma in situ showing no immunoreactivity to PA2.26 Ab. A stained lymphatic vessel (lv) in the edge of the tumour serves as a positive control. (*c*, *d*) Hyperplastic mucosa adjacent to a SCC weakly stained for PA2.26 showing strong PA2.26 immunoreactivity in the basal layer. Panel *d* shows a higher magnification of the region marked in panel *c*; tn, tumor nest; e, epithelium. (*e*, *f*) Sections of a SCC (tongue) stained with PA2.26 (*e*) and E-cadherin (*f*) Abs. The tumour shows a strong PA2.26 staining in its invasive front (panel *e*), while E-cadherin is virtually absent from this area (panel *f*). (*g*, *h*) Sections of a SCC showing patchy and heterogeneous PA2.26 (*g*) and E-cadherin (*h*) staining. PA2.26 is mainly concentrated at the plasma membrane

of carcinoma cells in contact with the stroma (*g*), while E-cadherin staining tends to be suprabasal (*h*).

Figure 5. Confocal immunofluorescence colocalization of PA2.26 with E-cadherin (*b-d*) and ezrin (*f-h*) in OSCCs. Panels *b-d* and *f-h* show fluorescence localization of the indicated proteins in tumour sections. Colocalization is visualized by yellow colour. Panels *a* and *e* show PA2.26 immunohistochemical staining of sections from the same tumours as in *b-d* and *f-h*, respectively. Note in panels *b-d* reduced or absent E-cadherin staining in carcinoma cells expressing PA2.26. Insets in these panels show a tumour region which is negative for PA2.26 staining and exhibits normal E-cadherin expression. Arrowhead in panel *e* indicates the zone showed in panels *f-h*. Note in panels *f-h* that PA2.26 colocalizes with ezrin at the plasma membrane of carcinoma cells. Some PA2.26-stained, ezrin-negative cells are also seen in the stroma. Insets in panels *f-h* show a higher magnification of the area marked with asterisk. Bars, 20 μm.

Figure 6. Confocal immunofluorescence localization of human PA2.26 and ezrin in HeLa and HaCaT cells transiently transfected with PA2.26 cDNA. (*a*, *b*) Maximum projections of horizontal (xy) optical sections through the whole depth (*a*) or the apical domain (*b*) of HeLa and HaCaT cell transfectants, respectively, stained with PA2.26 Ab. (*c*, *f*) Vertical (xz) optical sections obtained in panels *a* and *b* (discontinuous line), respectively. Note PA2.26 localization at plasma membrane protrusions. (*e-j*) Immunofluorescence colocalization of PA2.26 and ezrin in HeLa (*e-g*) and HaCaT (*h-j*) cell transfectants. Three-dimensional projections of confocal horizontal sections made in PA2.26 (green) and ezrin (red) stained cells are shown. PA2.26 and ezrin colocalize (yellow) at plasma membrane protrusions in reconstructions of dual colour horizontal

sections (*c* and *j*). Note a clear redistribution of ezrin to the cell borders in transfected cells. Many PA2.26-containing protrusions (arrows) have lengths $\geq$ 8 μm resembling filopodia (insets in panels *e-g*), while ezrin in PA2.26 non-expressing cells decorates microvilli or microspikes. Nuclei were stained with DAPI. Bars, 20 μm (*a*, *b*, *h-j*); 8 μm (*e-g* and insets).

Figure 7. Confocal immunofluorescence localization of E-cadherin and β-catenin in HaCaT-EGFP (*a-d*) and HaCaT-PA2.26-EGFP (*e-h*) stable transfectants grown at confluence. Panels *a* and *e* show phase contrast micrographs of HaCaT keratinocytes transfected with EGFP (Ha-EGFP) and PA2.26-EGFP (Ha-2.26-EGFP) fusion construct, respectively. Panels *b-d* and *f-h* show fluorescence localization of the indicated proteins in cells fixed in methanol (in order to better visualize E-cadherin and β-catenin staining), except for cells in inset of panel *b* that were fixed in formaldehyde (in order to see EGFP subcellular localization). EGFP is distributed uniformly through the cytoplasm as a soluble protein (panel *b* and inset) that is eliminated in cells fixed in methanol (panel *b*). Insets in panels *c*, *d*, *g* and *h* show higher magnifications of cell-cell borders. E-cadherin and β-catenin were detected by indirect immunofluorescence using specific mAbs. PA2.26-EGFP is directed to the plasma membrane and membrane protrusions (*f* and inset). Note perturbed distribution of E-cadherin and β-catenin with presence of the proteins out of cell-cell contacts in PA2.26-EGFP with respect to EGFP transfectants. Bars, 100 μm (*a*, *e*), 40 μm (*b-d*, *f-h*).

Figure 8. Expression of PA2.26-EGFP inhibits E-cadherin function in HaCaT keratinocytes. (*a*) Expression of PA2.26-EGFP and E-cadherin proteins in parental cells, EGFP transfectants (Ha-EGFP-c7) and PA2.26-EGFP transfectants (Ha-2.26-

EGFP-p6, -p7, -c7, -c11) by Western blotting using PA2.26 Ab and a specific anti-E-cadherin mAb. The filter was reblotted with an anti-α-tubulin mAb as a control for protein loading. (*b*) Ca^{2+}-dependent cell aggregation in HaCaT and transfectant cells as shown by the aggregation index determined after 60 minutes of incubation in the presence of 10 mM Ca^{2+}, as described in Materials and Methods. The aggregation index is expressed normalized to that obtained in the presence of EGTA. (*c*) Phase contrast micrographs of cell aggregates obtained after 60 min of incubation in the absence (EGTA) or presence of Ca^{2+}. Bars, 100 μm.

TABLE 1 – EXPRESSION OF PA2.26 IN HUMAN ORAL SQUAMOUS CELL CARCINOMAS

Site	Cases	Number of cases showing positive reactivity to PA2.26 antibody
Floor of mouth	26	8 (31%)
Tongue	35	7 (20%)
TOTAL	61	15 (25%)
Stage I[a]	22	4 (18%)
Stage II	39	11 (28%)
WD[b]	27	7 (26%)
MD	34	8 (24%)

[a]Stage 1: T1, tumor 2 cm or less in greatest dimension; N0, no regional lymph node metastasis; M0, no distant metastasis. Stage II: T2, tumor size between 2 to 4 cm; N0; M0.
[b]WD, well differentiated; MD, moderately differentiated

A

```
   1                                                                                                  CAACTGCAAAGTTTGCTGTCCGGCTGCCT
  30  AGGGTCTGGGAAGCTCGGGCACCCTCCCTCTCCGGGGCTCCTGCTCCCACCCCTCCGGCCCCTCCACCGTCGCGCTCCTCCAGGCTG
 117  GGCCTGTGGCCGCGGTGCTTTTTAATTTTCCCCCAGCTCAGAATCTTGCTGCTCGGCCCCCAGGAGAGCAACAACTCAACGGGAACG

      Met Trp Lys Val Ser Ala Leu Leu Phe Val Leu Gly Ser Ala Ser Leu Trp Val Leu Ala Glu Gly   22
 204  ATG TGG AAG GTG TCA GCT CTG CTC TTC GTT TTG GGA AGC GCG TCG CTC TGG GTC CTG GCA GAA GGA

      Ala Ser Thr Gly Gln Pro Glu Asp Asp Thr Glu Thr Thr Gly Leu Glu Gly Gly Val Ala Met Pro   44
 270  GCC AGC ACA GGC CAG CCA GAA GAT GAC ACT GAG ACT ACA GGT TTG GAA GGC GGC GTT GCC ATG CCA

      Gly Ala Glu Asp Asp Val Val Thr Pro Gly Thr Ser Glu Asp Arg Tyr Lys Ser Gly Leu Thr Thr   66
 336  GGT GCC GAA GAT GAT GTG GTG ACT CCA GGA ACC AGC GAA GAC CGC TAT AAG TCT GGC TTG ACA ACT

      Leu Val Ala Thr Ser Val Asn Ser Val Thr Gly Ile Arg Ile Glu Asp Leu Pro Thr Ser Glu Ser   88
 402  CTG GTG GCA ACA AGT GTC AAC AGT GTA ACA GGC ATT CGC ATC GAG GAT CTG CCA ACT TCA GAA AGC

      Thr Val His Ala Gln Glu Gln Ser Pro Ser Ala Thr Ala Ser Asn Val Ala Thr Ser His Ser Thr  110
 468  ACA GTC CAC GCG CAA GAA CAA AGT CCA AGC GCC ACA GCC TCA AAC GTG GCC ACC AGT CAC TCC ACG

      Glu Lys Val Asp Gly Asp Thr Gln Thr Thr Val Glu Lys Asp Gly Leu Ser Thr Val Thr Leu Val  132
 534  GAG AAA GTG GAT GGA GAC ACA CAG ACA ACA GTT GAG AAA GAT GGT TTG TCA ACA GTG ACC CTG GTT

      Gly Ile Ile Val Gly Val Leu Leu Ala Ile Gly Phe Ile Gly Gly Ile Ile Val Val Val Met Arg  154
 600  GGA ATC ATA GTT GGG GTC TTA CTA GCC ATC GGC TTC ATT GGT GGA ATC ATC GTT GTG GTT ATG CGA

      Lys Met Ser Gly Arg Tyr Ser Pro Stop                                                       162
 666  AAA ATG TCG GGA AGG TAC TCG CCC TAA AGAGCTGAAGGGTTACGCCCTGCTGCCAACGTGCTTAAAAAAAGACCGTTT

 744  CTGACTCTGTGCCCTGTCCCTGAGCTCGTGGGAGAAGATGACCCGTGGAACACTTGCCTGGCCCACTCAGAATCCACGGTGACCTCT
 831  CCGCTTGCCAAAATAACCGAAGGAAAGACCGTTCACCAGACTTGGCTCCTCTAAACATTTGCTGTTCAAACATGTTTTTGAATATAC
 918  ATTCTATAAAAGATTATTTGAAAGACAAAATTCATAGAAAATGGAGCAAAACTGTATAAACTGATTTGTAACTAACACTGGACCATT
1005  GGATCGATATTATATGCTGTAACCATGTGTCTCCGTCTGACCATTCTTGTTATTGTTAAAATGCAGAGGAATCTGGAAATATTTATA
1092  TCCACGGAGTCCTTGGATCCAGTGCTACGTCAGTAAATAGCACCAGCATTTTGCAATTGCTGATCTGCTGAAATGTACACATTCTGG
1179  TCTAGTTTGGTCTATCTTTTAAAGCCTGATCTGGTGTGAATAATCAACTAGGAAATCTAAACTTGGATAACACGTGGTGAACAACTG
1266  CCTTTAGCTGGTCCAGATTAATCATTTCAAAGACATCCATTTTAGATCACAAGCAGGAAGTCGATAGTCTCAAAGGCACTTTGTTTC
1353  TCCCAAGTAGGCCACCAGGCAGCCTCTAGAGTTGCTTTACCCAAATCCTTCTCCAGCCATGACTTGGTGACTCTAAGCTTGCTCCCA
1440  CCTGCCCCCTCCACTTCCCTCAGATGATGAGGAGCCAGGGCTAAGGGGGCAGCCTTCTCTCTTCCCAGTGATGCACATCCTTCACAT
1527  TGGCTGCTTTGTTCTGGAATATGGATATCTCAGCCTGGATGCCGAGGAAGCTGCTGGATGCTTAATGGTGCTAGAGGCTCAAGTGTG
1614  TTTGAAACCAAGAGCCAGTTGTCCCCCATGCAGAAAGAAATCCTGTGTGAGCCTCTGGTATGAGAAATAAAATCTGCCAGTTTTATA
1701  ACATTCACTTTCTGCCTCTGAGGAAAGATACAGGGAACAAAAATCAATTTGTACAGTCTTAATATTAAAAGCAGCTTGACTAAATAC
1788  CTGATTTAAAAATAGAAGACATCCCCAGTCCTCATGACATACCGCAAATATCTGTGGGGTCCTGTTGAAAAGAACAAAATAAAGGAG
1875  CCCAAGGGGTCATTCTGTCTCAGCACCATCCAGCCTGGCACTTCTCTTCCCATATATCCATTGGATTTTTTTTTTTTTCCTAAACA
1962  AAGTTTTTACACTGAGCAGATGCTCTGTCATGATGGCGGTTGTGCAATTCTGGTATCCTCTAAATTTGTAAGCATTCATAAAACAGG
2049  AAAAAGTAAACTATCATTCGGAAGCACAGCCCATTCCTCCCATTTTTTGCAATGATGTCTGGATGTTATTTTAAACAGTGTGTCTGT
2136  GTGTTCCCAAATCCAGCTGGCCCCACCAGCTCAGATTCCATTTTTTTTTGTGTGTGTGTGTGAAACGTAGTCTGCAACTCTGCCTCCC
2223  GGCAATTATACATGTGTCAGGATGTCAA***AAAGCAATTCTCCTGCCTCAGCCTCCTGAGTAGCTGGGACTACAGGTTCCTACCACCAC***
2310  ***ACCCGGCCAATTTTTGTATTTTTAGTAGAGATGGGGTTTCACCGTATCGGCGAGGATGATCTCTATCTCTTGACCTCGTGATCTGCC***
2397  ***CGCCTCGGCCTCCCAAAGTGCTGGGATTACAGGCGTGTGCCACTGCGCTCGGCCT***CAGATTCCATATTTGAACACCAGCTGATTGAG
2484  AGAAGGGGAATGAGAAGAGCTGGATGAGTTTAAATAACTCATTGTTCAGATTCCTGAACAGGAGTTGGGATAATGGCCATCTTTTCT
2571  TTCCTATCCTTTCTTCCCCCCTCACTGTGAAAAATAACAGTCCACCCCAAGTCATACACTGGACCCAGTGCCTGCGGGGACAGGACT
2658  GTGGGTTTCTTGGTCACACCTGTGTTGGTGCTCAATGCAGTGTAGACATGTTTTCA**AATAAA**ACAAATGATTGTGTACAA
```

B

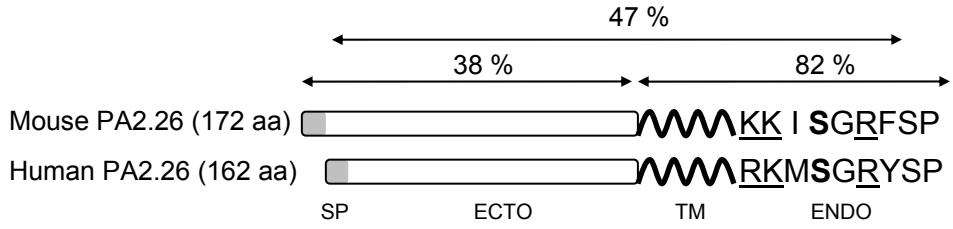

C

Martin-Villar et al. Figure1

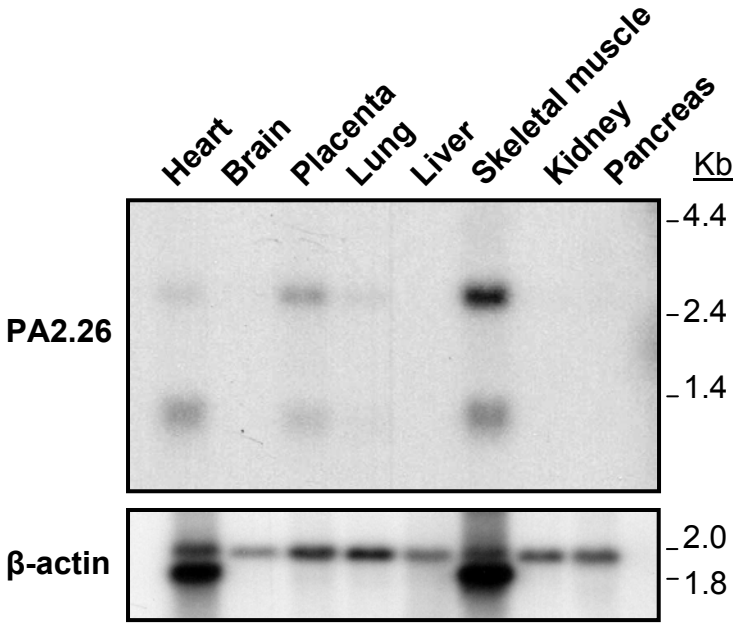

Martín-Villar et al. Figure 2

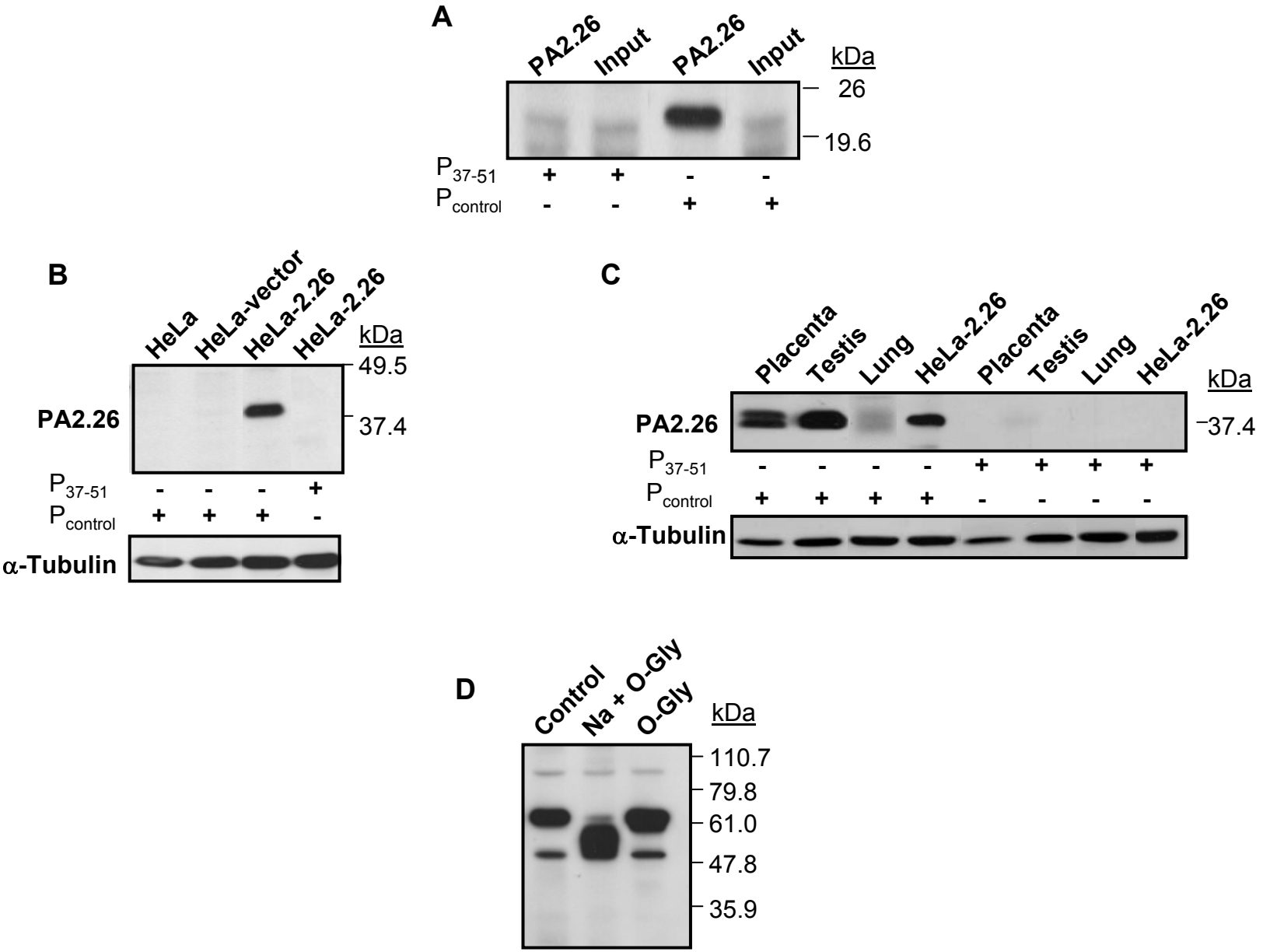

Martin-Villar et al. Figure 3

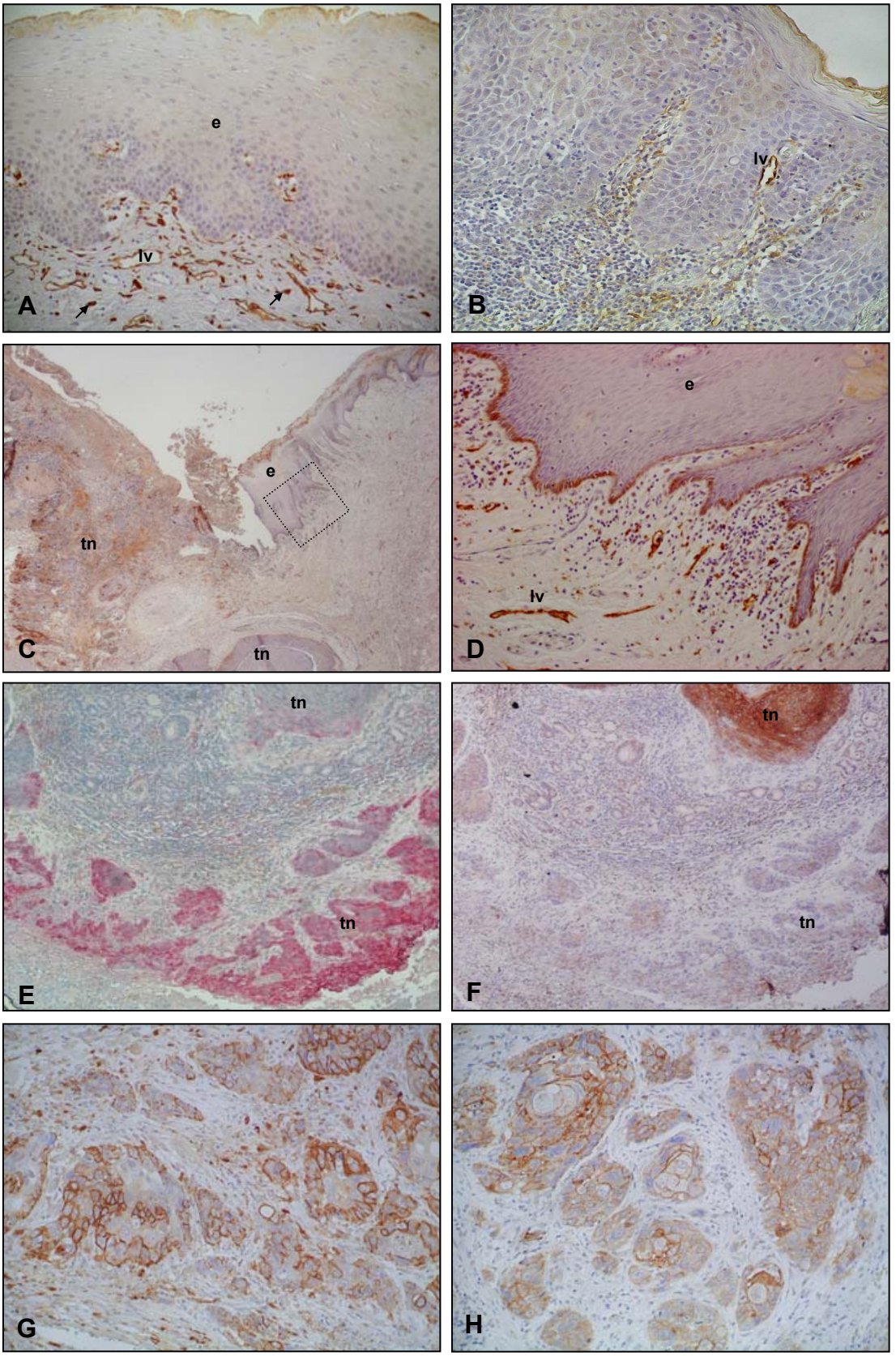

Martín-Villar et al. Figure 4

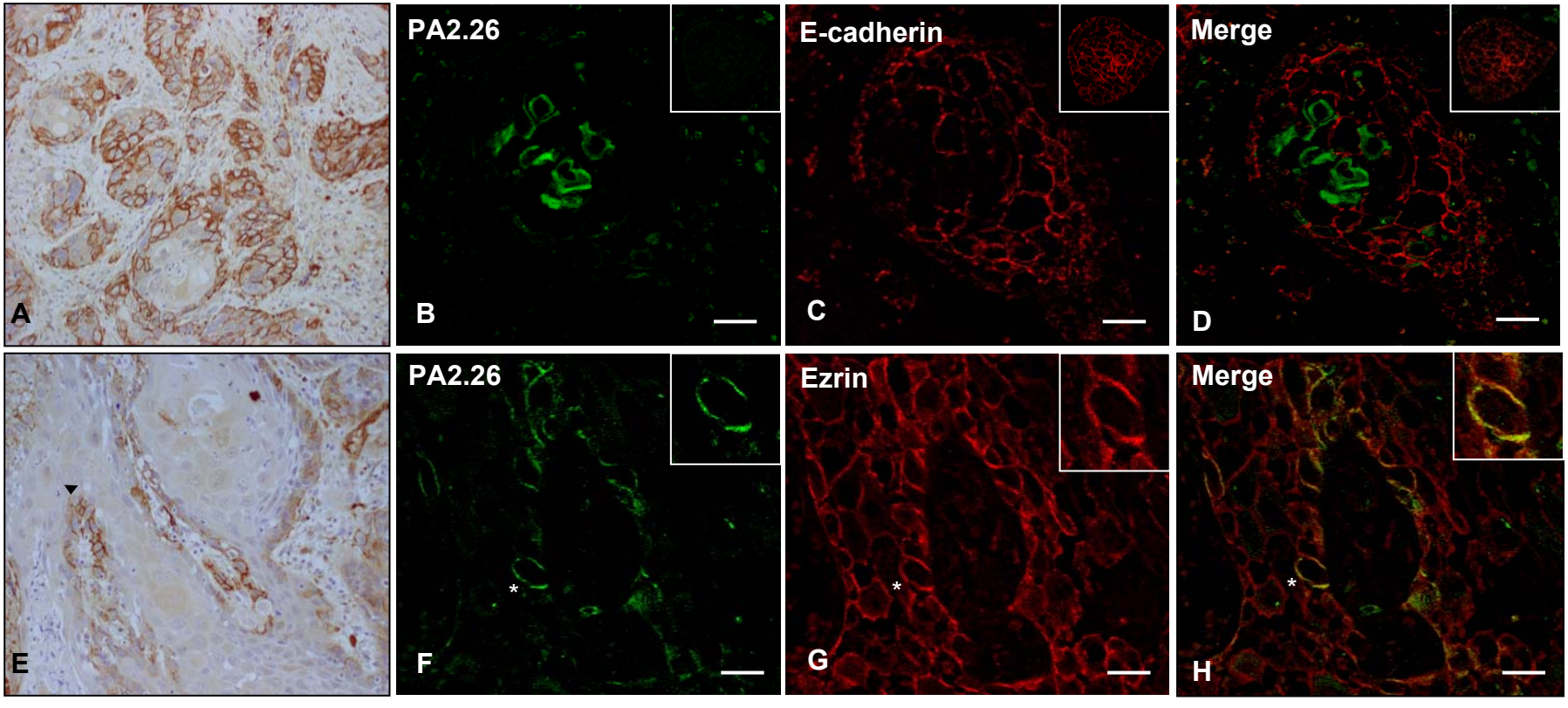

Martín-Villar et al. Figure 5

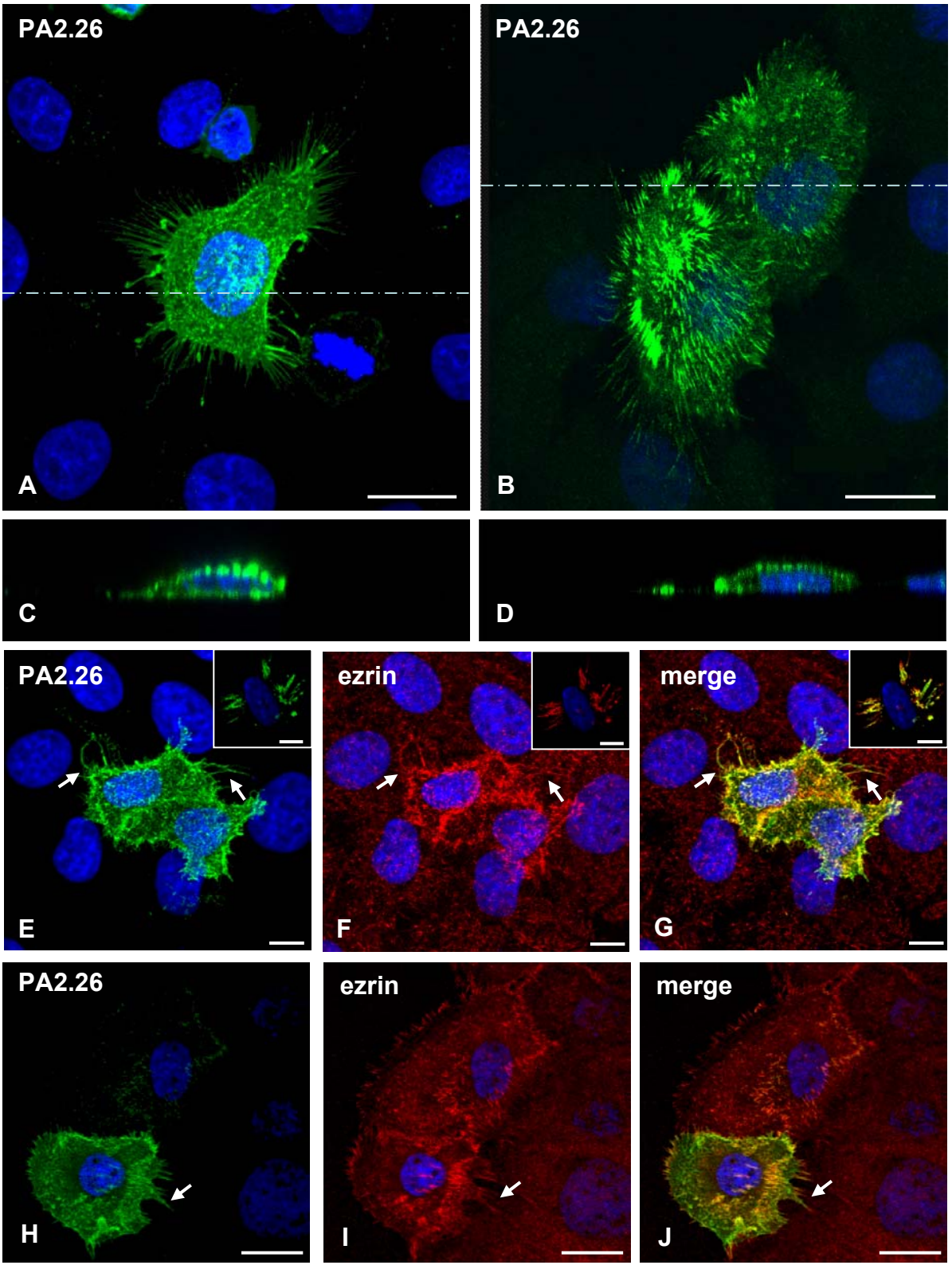

Martin-Villar et al. Figure 6

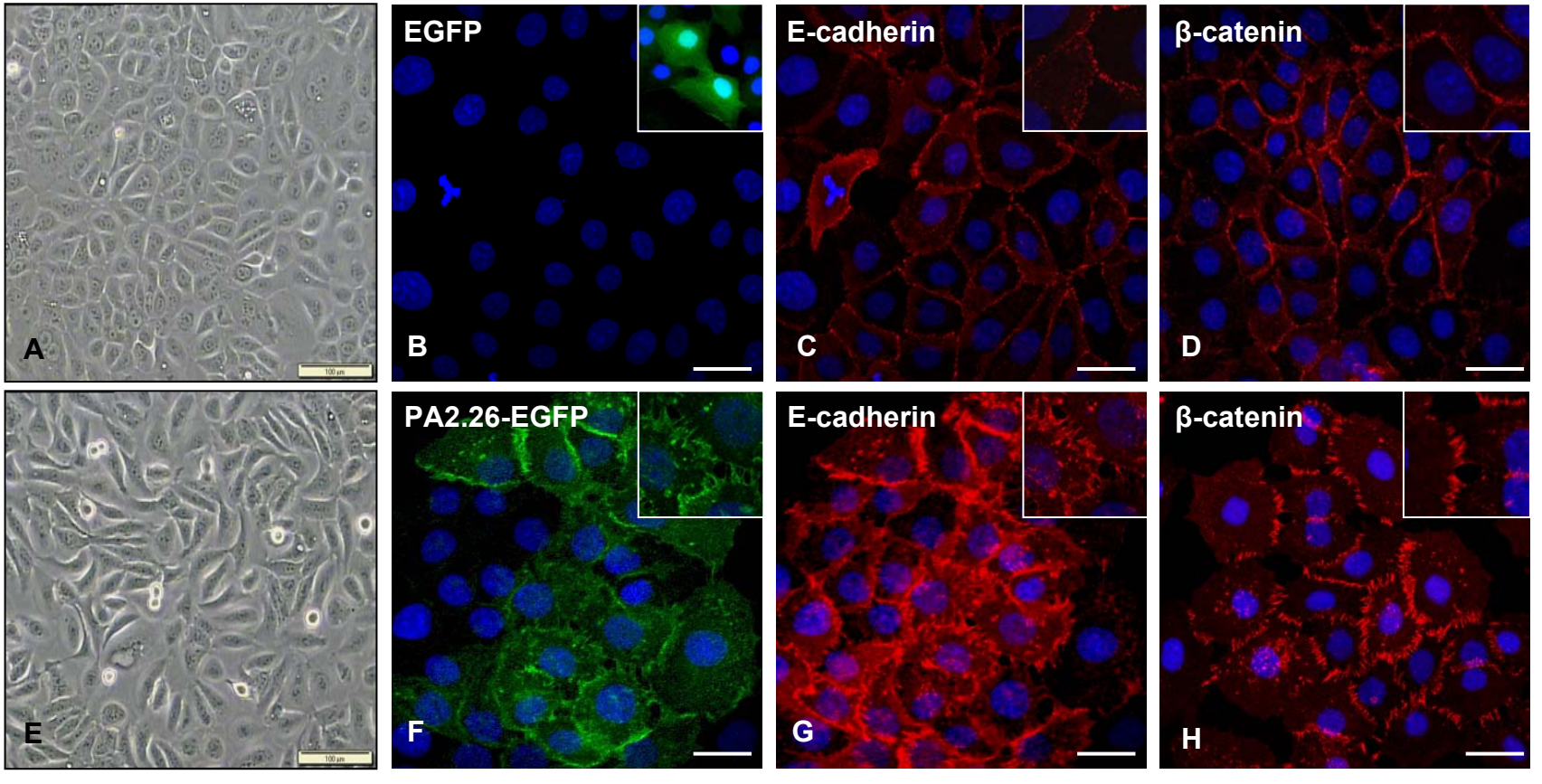

Martin-Villar et al. Figure 7

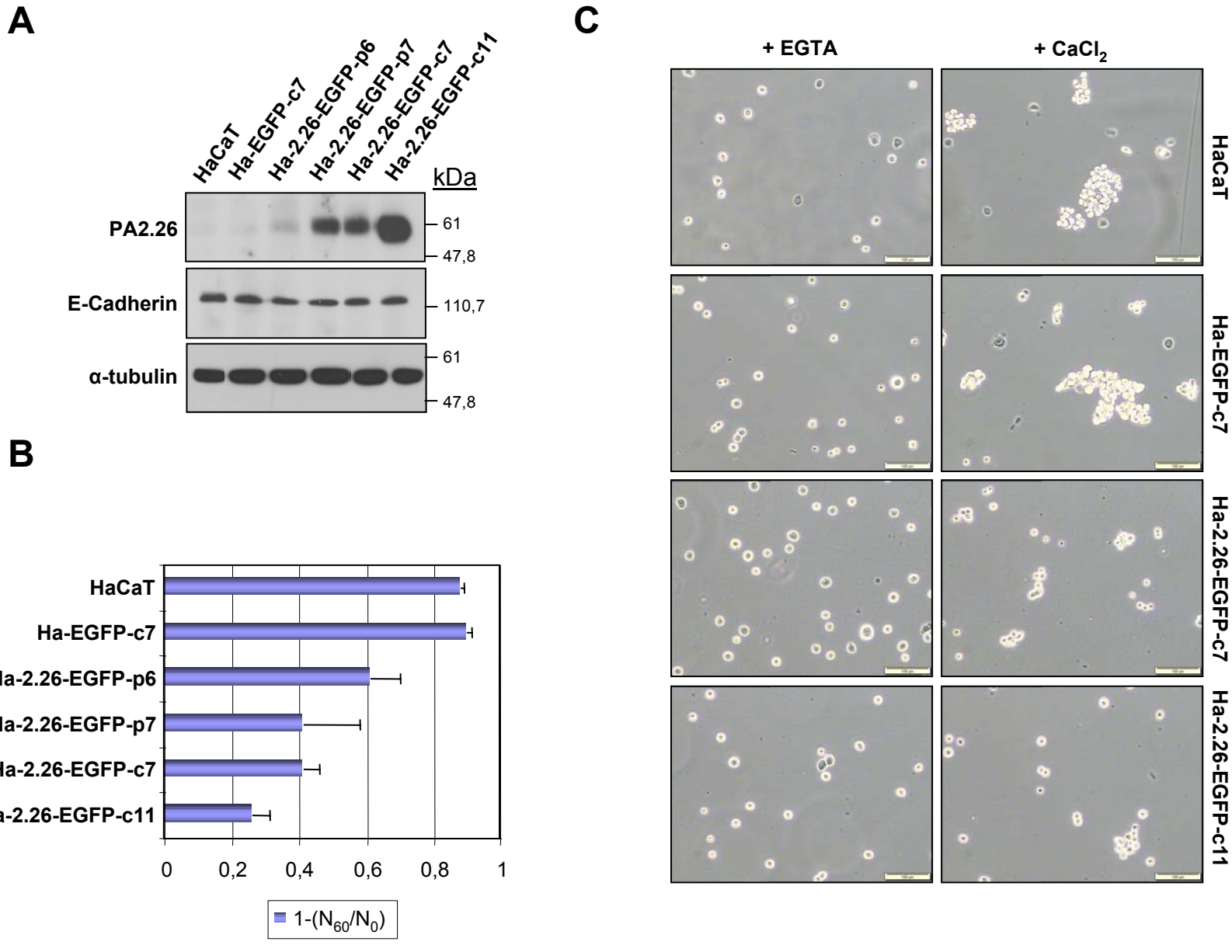

Martin-Villar et al. Figure 8